Charge Transport and Relaxation in Triglycine Sulphate (TGS)

W. Osak

Institute of Physics and Computer Science, Pedagogical University, ul. Podchorążych 2, 30084 Kraków, Poland

Z. Naturforsch. **52a**, 621–628 (1997); received February 17, 1997

Charging currents, $J-V$ characteristics and electron conductivity have been measured in triglycine sulphate along three crystallographic directions: a, b and c. The measurements have been taken in a wide temperature range between $-196\,^{\circ}C$ and $80\,^{\circ}C$. It is found that the charging currents have short relaxation times in the directions: a and c and a long relaxation time along the ferroelectric b axis. The $J-V$ characteristics in the direction of the a and c axes have the shapes characteristic for linear dielectrics with space charge limited currents. The $J-V$ characteristic for the b axis depends on the temperature: In the region of the phase transition the Fridkin-Kreher formula ($J \propto V^{4/3}$) is satisfied; for low temperatures characteristic agrees with SCLC theory for linear dielectrics with Gaussian traps energy distribution.

The d.c. conductivity along the c axis is much higher than along the a and b axes. In the investigated temperature range, the electrical conductivity has an activation character. For $-100\,^{\circ}C < T < -193\,^{\circ}C$ there is: $\sigma \propto (1/T)\exp(-E/kT)$. The activation energy depends both on the crystallographic direction and on the temperature-range. For low temperatures, $T < -100\,^{\circ}C$, the activation energies are very small (of the order of a few hundreds eV).

Key words: Ferroelectrics, $J-V$ characteristics, Electrical conductivity.

Subject classification: 72 (Electronic transport in condensed matter); 77 (Dielectrics, piezoelectrics and ferroelectrics and their properties).

1. Introduction

The electrical conductivity of triglycine sulphate has been studied by many researchers [1–5]. Most measurements were perfomed close to the ferro-paraelectric phase transition (between 20 and 80 °C). In [5], the electrical conductivity has been investigated from $-196\,^{\circ}C$ to $120\,^{\circ}C$ for the sample oriented perpendicular to the ferroelectric b-axis.

In this work, we supplement our previous results with the studies of the electrical conductivity between -196 and $120\,^{\circ}C$ along the non-ferroelectric a- and c-axes. The measurements have been performed in a way allowing to minimise the influence of non-linear effects.

In ferroelectrics, the current depends not linearly the voltage [5–7]. Additionally, relaxation currents appear [8], i.e. the current may become constant after some time (relaxation time). The relaxation time depends on temperature and electric field strength.

Reprint requests to Mr. W. Osak.

2. Theory

2.1 The Current-Voltage Characteristics

In dielectrics and semiconductors, the relation between applied voltage and current may be very complicated. When space-charge limited currents appear, the relation between the current density J and the voltage V depends on:

(1) the concentration of the injected and thermal equilibrium charges;
(2) the concentration N_t and energy E_t of traps levels.

The $J-V$ characteristics have been analyzed for solids with various trap energies. Most frequently analyzed were: traps confined in single or multiplet discrete energy levels, traps distributed exponentially, traps distributed Gaussianly and traps distributed uniformly within the forbidden energy gap [9].

For dielectrics with single discrete energy levels E in the range of weak voltages, Ohm's law is fulfilled. For higher voltages, when the concentration of injected charges prevails, the Mott-Gurney law holds [9]:

$$J = \frac{9}{8} \cdot \Theta \varepsilon \mu V^2 d^{-3} . \tag{1}$$

0932-0784 / 97 / 0800-0621 $ 06.00 © – Verlag der Zeitschrift für Naturforschung, D-72027 Tübingen

The coefficient Θ in (1) denotes the ratio of free charges to total charges (free and trapped); $\Theta = 1$ for dielectrics without traps and $\Theta < 1$ for dielectrics with traps. From the value of the voltage V_p which separates Ohm's from Mott-Gurney range, one can calculate the mobility and concentration of the thermal equilibrium free charges [9]. The trapps' concentration N_t may be calculated from the traps-filled-limit-voltage V_{TFL} [9].

In organic molecular crystals two types of the carrier trap distribution have been reported. They are: (1) the traps are confined in discrete energy levels in the forbiden energy gap and (2) the traps show a quasi-continuous distribution of energy levels, having a maximum trap density near the band edges.

Some general considerations have been suggested: to relate discrete trap levels with chemical impurities (chemical traps) and to relate a quasi-continuous distribution with the imperfection of the crystal structure (structural traps) [10–12].

For molecular crystals several investigators [13, 14] have proposed that some types of traps can better be described by a Gaussian distribution function

$$N(E) = \frac{N_t}{\sqrt{2\pi}\sigma} \exp\left[-\frac{(E - E_t)}{2\sigma^2}\right], \tag{2}$$

where E_t is the trap energy level with the maximum trap density σ. In [13] the validity range for various approximations has been determined by comparison of numerical integration and analytical approximation data. Generally, for a Gaussian distribution of local states the approximation $J \sim V^{m+1}/d^{2m+1}$ is valid, where $m = d(\ln J)/d(\ln V)$. m increases with increasing voltage from $m = 2$ to $m = 3$.

The problem of space-charge limited currents in ferroelectrics is more complicated than for linear dielectrics. The following facts should be considered:

(1) the dielectric polarization is not a linear function of the applied electric field
(2) the dielectric permittivity is strongly dependent on the temperature and applied electric field
(3) dielectric hysteresis occurs.

For ferroelectric crystals with a second order phase transition the following results were obtained by Fridkin and Kreher [6]:

1. for weak electric fields, Mott-Gurney-Child's law is true: $J \sim V^2/d^3$,
2. for strong electric fields, the relation

$$J = 0.53 \cdot \mu \cdot \xi^{-1/3} V^{4/3} d^{-7/3}$$

holds, where: J = current density, ξ = Devonshire coefficient and d = sample thickness. These relations are true in the vicinity of the Curie temperature.

2.2 Charge Carrier Transport in Molecular Crystals

The electrical conductivity is given by

$$\sigma = n e \mu, \tag{4}$$

where μ denotes the carrier mobility and n the density of free carriers.

Solid dielectrics are pour conductors; i.e., n and μ are small. Low mobility arises from weak electron transfer (narrow bands) or (and) strong electron-phonon coupling. Low density of current carriers results from a wide band gap separating a full valence band from an empty conduction band.

The basic mechanism of charge transport in molecular crystals depends on the nature of the electron-exchange and electron-phonon interactions.

There are two limiting models which can provide convenient physical pictures of electrical transport in solids. These are: the band- and hopping-model. The criterion, allowing to determine whether the charge transport in a molceular crystal takes place coherently according to the band model or by random jumps according the hopping model, depends on the electron-lattice interactions.

The experimental fact that the temperature dependence of the mobility follows the relation $\mu = C T^{-n}$ (where $0 < n < 2.5$) has led to the development of the band theory for the carrier transport in molecular crystals.

However, there is some evidence that electron-phonon interactions are strong in molecular crystals, and the carrier transport may be better described by a type of hopping motion whit the mean free path of the order of a lattice constant.

The interaction of electrons and phonons in a lattice site may lead to self-trapping in which the electrons polarize the molecules and are trapped in self-induced potential wells. The combination of an electron and its induced polarization field is called a polaron. For molecular crystals it is most likely the polarons are small and strongly coupled. The hopping transport takes place if the electron-phonon interaction is strong. The drift velocity of charge carriers is determined by interaction with phonons and their energy spectra. The electrical transport at room temperature for most organic molecular crystals is intermediate

between band-type transport and small polaron hopping transport. Charge carrier transport in molecular crystals was described in review papers [15–16] and monographs [9, 17].

The temperature dependence of the mobility of small polarons is a function which involves the quantities describing the mechanism of electron-phonon coupling [9, 15–20].

3. Samples and Method

Spectrally pure sulphate acid and glycine, taken at stoichiometric proportion, were used to obtain triglycine sulphate, TGS $(NH_2CH_2COOH)_3\,H_2SO_4$. The triglycine sulphate single crystals were grown by decreasing the temperature of an aqueous solution purified by double recrystallization. The crystals were transparent and optically homogeneous.

The samples for the measurements (thickness 1.2 mm, surface area 0.64 cm^2) were covered with golden electrodes evaporated in vacuum. All samples had a guard ring. The samples were oriented perpendicular to the principal crystallographic directions: *a*, *b*, and *c* using an X-ray diffraction method. Before every measurement the samples were held for one hour at 80 °C. A description of an experimental set and the method of measurements may be found in [5, 8].

4. Results

4.1 Charging Currents

Figure 1 shows the time dependence of the charging current $J_C(t)$ for three samples in the direction of the principal crystallographic axes *a*, *b*, and *c*. In the samples polarised in the direction of the ferroelectric *b* axis a very slow relaxation current flows, which reaches a steady-state value after about 10^4 s. For non-ferroelectric *a*- and *c*-axes the relaxation time is shorter and equals about 10–15 min.

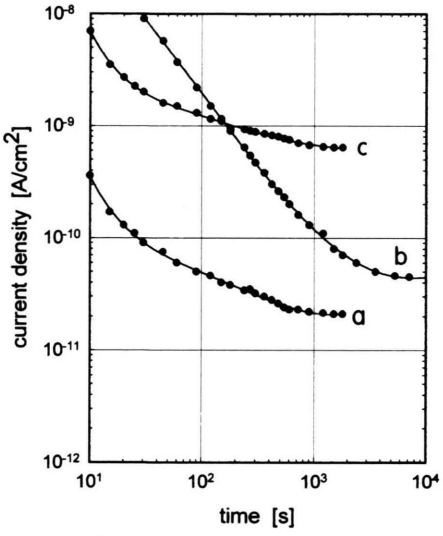

Fig. 1. TGS. Charging currents measured at 25 °C in the direction of the crystallographic *a*-, *b*-, and *c*-axes. Polarisation voltage 100 V, sample thickness 1.2 mm.

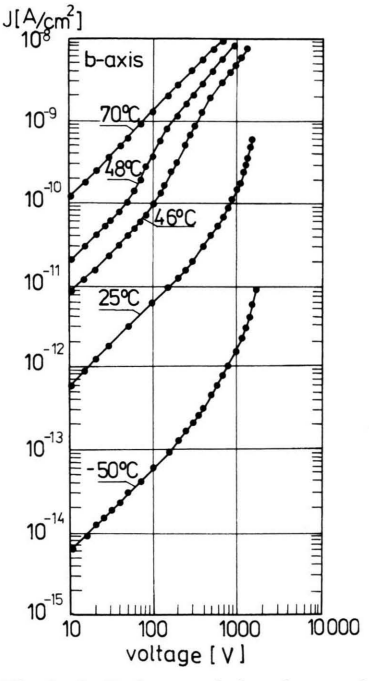

Fig. 2. *J*–*V* characteristics of a sample orientated along ferroelectric *b*-axis.

4.2 Current-Voltage Characteristics

The steady-state values of the current have been used to plot the current-voltage characteristics.

Figure 2 shows the *J*–*V* characteristics for the sample orientated along the crystallographic *b*-axis (ferroelectrics *b*-axis). At 46 °C and 48 °C (Curie temperature 49.3 °C) the *J*–*V* characteristics follow Ohm's at low voltages. For higher voltages, the square law $J \sim V^2$, followed by the Fridkin-Kreher relation $J \sim V^{4/3}$, is true. The same relation is characteristic for the space charge limited current (SCLC) flowing in

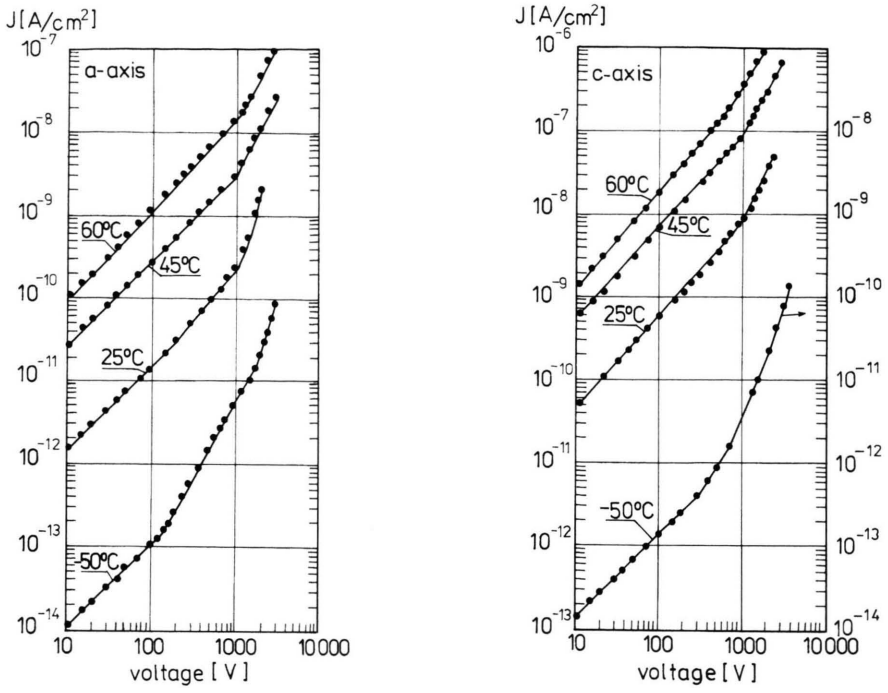

Figs. 3a and b. TGS. $J-V$ characteristics of samples oriented in the a and c crystallographic directions. The sample thickness 1.2 mm.

Table 1. Free charge carrier mobility and concentration measured along three crystallographic directions at various temperatures.

T [°C]	μ [m²/V s] Crystallographic direction			n [m⁻³] Crystallographic direction		
	a	b [1]	c	a	b [1]	c
48	–	$1.8 \cdot 10^{-11}$	–	–	$5.5 \cdot 10^{18}$	–
46	–	$9.8 \cdot 10^{-12}$	–	–	$4.3 \cdot 10^{18}$	–
25	$1.6 \cdot 10^{-10}$	$2 \cdot 10^{-13}$	$6.3 \cdot 10^{-9}$	$3.5 \cdot 10^{17}$	$3.4 \cdot 10^{17}$	$3.6 \cdot 10^{17}$
−50	$4.5 \cdot 10^{-12}$	$2 \cdot 10^{-14}$	$5.5 \cdot 10^{-12}$	$8.3 \cdot 10^{17}$	$9.6 \cdot 10^{16}$	$8.6 \cdot 10^{16}$

[1] See [5].

ferroelectrics with second order phase transition [5, 6]. At − 50 °C, for low voltages Ohm's law is fulfilled, followed by the square law. Furthermore, a strong increase of the current for the high voltages can be seen on the characteristics measured at 25 and − 50 °C.

Figures 3a and 3b show the $J \sim V$ characteristics for samples orientated along the non-ferroelectric crystallographic a and c axes. In the range of low voltages Ohm's law is fulfilled, followed by a square dependence $J \sim V^2$. A strong increase of current occurs for high voltages.

The concentration and effective mobility of the charge carriers have been calculated.

The results, which are shown in Table 1, indicate what follows:

- The carrier mobility depends on the crystallographic orientation. It is greater for the direction of the c-axis than of the ferroelectric b-axis.
- The carrier mobility and concentration increases strongly with increasing temperature.
- The trap concentration evaluated from the experiment is about $8.9 \cdot 10^{17}$ m^{-3}.

It should be stressed that the effective mobilities estimated according to (3) are very rough approximations, and that the very low values of μ are caused by effective carrier trapping phenomena.

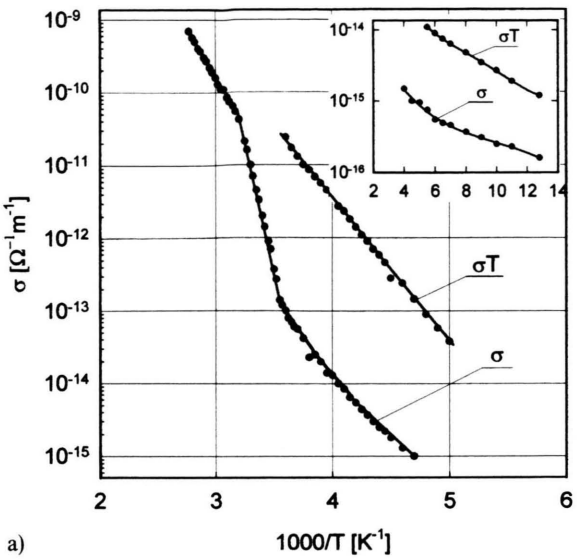

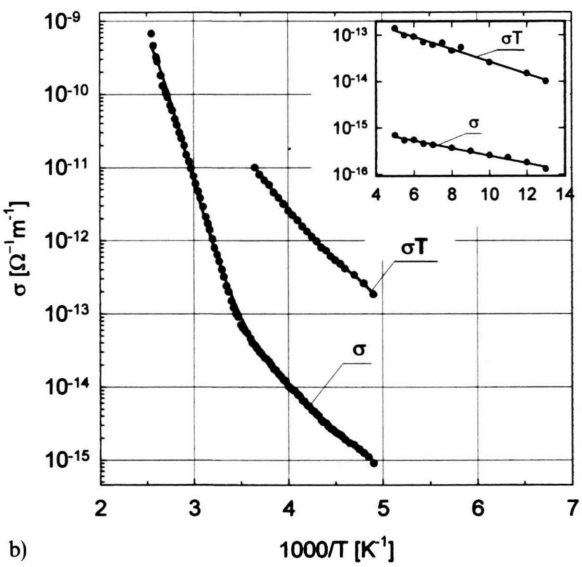

Fig. 4a and b. Temperature dependence of electrical conductivity σ. In inserts: σ versus $(1/T)$ for low temperatures. a) σ in the direction of the a-axis. b) σ in the direction of the c-axis.

4.3 Electrical Conductivity

Figures 4a and b show the temperature dependence of electrical conductivity from −196 to 120 °C for samples orientated in the crystallographic a- and c-axes. From the $J-V$ characteristics it results that the range of voltages where Ohm's law is valid, decreases with decreasing temperature (e.g. for a-axis, this value decreases from 1000 V at 60 °C to 30 V at − 50 °C).

The respective values of the electrical conductivity in the samples orientated along ferroelectric b-axes can be found in [5].

Table 2 presents activation energies of electrical conductivity measured for the a-, b- and c-axes. It is clear that these values depend on the orientation of the crystal and the temperature.

5. Discussion

1. Strong relaxation currents in addition to non-linear properties of TGS make the measurements of the electrical conductivity in the samples oriented perpendicular to the ferroelectric b-axis difficult. The mentioned effects do not disturb the measurements in the direction of non-ferroelectric a- and c-axes. In the experiment, in order to reach the steady-state current in a short period of time, it is necessary to apply a strong electric field but not too strong to avoid injection of charges from the electrodes to the sample. For low temperatures this is a relatively small range of voltages, which can influence the accuracy of the measurements.

2. The shape of the characteristics (Figs. 2 and 3) indicates that for triglycine sulphate a Gaussian distribution of trap energies may be proposed, since

a) the slope m of the $J-V$ characteristics increases with increasing voltage and
b) m increases with decrease of temperature.

a-axis	T [°C]	−196 ÷ −110	−110 ÷ 10	10 ÷ 49	49 ÷ 100	100 ÷ 120
	E_a [eV]	0.025	0.32	0.97	1.40	–
b-axis	T [°C]	−196 ÷ −110	−110 ÷ 10	10 ÷ 49.5	49.5 ÷ 80	80 ÷ 120
	E_a [eV]	0.028	0.29	1.6	0.97	1.95
c-axis	T [°C]	−196 ÷ −110	−110 ÷ 10	10 ÷ 49	49 ÷ 80	80 ÷ 120
	E_a [eV]	0.033	0.41	1.23	0.52	–

Table 2. Activation energies calculated from d.c. conductivity measurements in TGS along the three crystallographic directions.

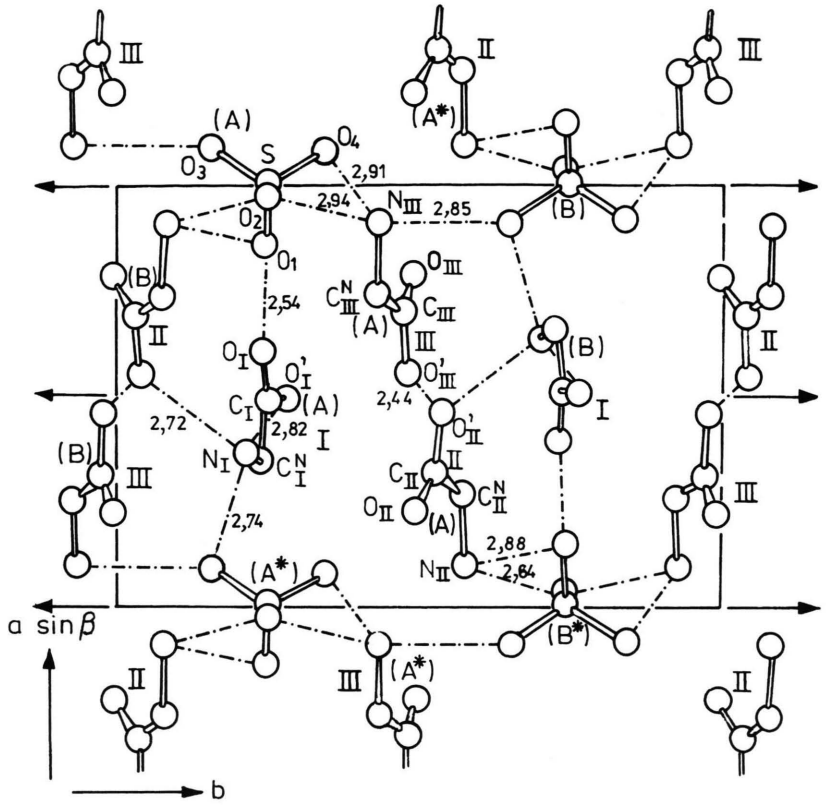

Fig. 5. Projection of the glycines and the SO_4^- ions on the plane (001). The structure according to Hoshino et al. [25].

In addition to the identified sources of traps in solids it can be expected that in triglycine sulphate single crystal there occurs new ones.

These new traps are connected with spontaneous polarization and the structure of the ferroelectric domains. In the neighbourhood of the domain wall there are sites at which the charge carriers are trapped. The energy of these trap levels equals approximately the energy of the deep traps. It is known that the spontaneous polarization decreases with increasing temperature; therefore the energy of traps originated from spontaneous polarization must decrease with the increasing temperature.

The $J-V$ characteristics measures in the vicinity of the Courie temperature (Fig. 2, curves 46 °C, 48 °C) show that the characteristic relation $J \sim V^{4/3}$, which is valid for ferroelectrics with second order phase transition, is fulfilled. At -50 °C the shape of the $J-V$ characteristics is practically the same as for linear dielectrics. It is know that at temperatures near Curie temperature great changes of the spontaneous polarisation take place. Therefore, in this range of temperatures ferroelectric properties predominantly affect the shape of the $J-V$ characteristics. At low temperatures, the shape of the $J-V$ characteristics is mainly determined by the number of traps and theirs energy distribution.

3. The carrier mobilities in TGS are very small and depend strongly on the temperature (see Table 1). Because of the high dielectric permittivity of triglycine sulphate, small polarons may be created [9, 17].

The triglycine sulphate single crystal (of the chemical formula: $(NH_2CH_2COOH)_3H_2SO_4$ has a monoclinic symmetry with two formula units per unit cell. Each formula unit contains three different glycine ions: GI, GII and GIII. The glycine GI ($NH_3^+CH_2COOH$) is non planar, while both GII (NH_3CH_2COOH) and GIII ($NH_3^+CH_2COO^-$) are planar. The NH_3 groups attached to GI, GII and GII rotate rapidly about the axis of C–C bonds. The rotation takes place both above and below the Curie temperature T_C. Nuclear spin relaxation studies have shown the existence of

both a "slow" reorientation proces associated with the strongly bonded NH_3 (II) and NH_3 (III) groups and a "fast" reorientation associated with NH_3 (I) [21]. Proton magnetic resonance [22, 23] has shown an anomaly around – 123 °C related to the slow process. Recent studies [24] have shown the existence of a phase transition at −163 °C. The vibration of the SO_4 group also shows a sudden change near −163 °C connected with the rotation of NH_3 groups of the glycines. Fast-rotating NH_3 groups cause a release of electrons which can move freely in the lattice. The configuration of the glycines and the SO_4 ions in the unit cell, shown in Fig. 5 [25], suggests a possible path of the electron transport in the lattice. In the direction of the *b*-axis, the carrier transport takes place through the hopping between GII, GI, GII, GI ... or through the hopping between the dipoles of glycine GII and the ion SO_4^-. The latter way of transport is less likely because of the long hopping distance as well as the big negative ion SO_4^-. The same situation appears if one considers a charge transport through the glycines GII and GI; the hopping distance between glycine GII and GI is comparatively long.

Quite different conditions of the hopping determine the transport in the direction of the *a*-axis. The hopping of the charge carriers takes place between the anion SO_4^-, the dipole of GIII and the GII ion. The charges can be also transported in another succession: through the glycines GIII, GII and the SO_4^- group. In both cases the big SO_4^--ions strongly influence the hopping of the electrons. In the direction of *c*-axis, the glycines GIII and GII constitute almost a planar structure. Furthermore, the influence of SO_4^- ions is much weaker. That is why in the direction of *c*-axis one should observe a much higher conductivity that in the direction of *a*- and *b*-axes (see Figs. 4a and b).

4. The fast increase of the electrical conductivity for the temperatures slightly lower than T_C may be explained through a disappearing of domain structure. The charges accumulated on the domain walls become free and may take part in the electrical transport. This effect is very distinct for low measuring voltages, but for higher voltages it has not been observed. A fast decrease of the electrical conductivity has ben observed for temperatures from −100 °C to the Curie temperature (see Figures 4a, b). It is known that low temperatures slow down the rotation of the NH_3 groups and the vibration of SO_4 groups [24]. As a consequence, this leads to the decrease of the electrical conductivity. For low temperatures, the electrical conductivity of TGS depends very weakly on the temperature (see Figs. 4a, b – inserts). At these temperatures, a tunnelling between sites of the carrier should be a more probable mechanism of the conductivity.

6. Conclusions

1. The dependence $J \propto V^{4/3}$, observed for the ferroelectric *b*-axis, confirms the presence of space-charge-limited currents in triglycine sulphate.

2. The temperature dependence of the electrical conductivity in TGS suggests a small polaron mechanism of the charge transport.

Acknowledgements

The author is grateful to Dr. P. Dobrzański from the Institute of Solid State Structure and Mechanics, Technical University of Mining and Metallurgy in Kraków, for performing the crystallographic orientation of the samples.

[1] H. Toyoda, T. Tanaka, and W. Shiokawa, Rev. Electric. Commun. Lab. **2,** 485 (1961).
[2] V. M. Gurevich, I. S. Zheludev, and I. S. Res, Kristallografiya **5,** 142 (1960).
[3] B. Hilczer and M. Michalczyk, Ferroelectrics **22,** 721 (1978).
[4] W. Osak and K. Tkacz, Ferroelectrics **81,** 53 (1988).
[5] W. Osak, K. Tkacz-Smiech, and C. Strzalkowska, Ferroelectrics **158,** 331 (1994).
[6] V. M. Fridkin and K. Kreher, Phys. Stat. Sol. (a) **2,** 281 (1970).
[7] W. F. Krapivin and E. W. Chensky, Fiz. Tverd. Tela **12,** 597 (1970).
[8] W. Osak and K. Tkacz, Phys. Stat. Sol. (a) **100,** 667 (1987).
[9] K. C. Kao and W. Hwang, Electrical Transport in Solids, Pergamon Press, Oxford, Chapt. 1 and 3 (1981).
[10] J. Sworakowski, Mol. Cryst. Liq. Cryst. **11,** 1 (1970).
[11] J. Sworakowski, Mol. Cryst. Liq. Cryst. **32,** 87 (1976).
[12] E. A. Silinsh, Phys. Status Solidi (a) **3,** 817 (1970).
[13] S. Nespurek and E. A. Silinsh, Phys. Stat. Sol. (a) **34,** 747 (1976).
[14] I. Gremet, C. Vautier, D. Carles, and I. I. Chabrier, Phil. Mag. **28,** 1265 (1973).
[15] E. A. Silinch, M. Bouvert, and J. Simon, Mol. Mat. **5,** 1 (1995).
[16] M. Bouvert, E. A. Silinsh, and J. Simon, Mol. Mat. **5,** 255 (1995).

[17] E. A. Silinsh and V. Capek, Organik Molecular Crystals. Interaction, Localisation, and Transport Phenomena, AIP Press, New York 1994.
[18] H. Bottger and V. V. Bryksin, Hopping Transport in Solids, Akademie Verlag, Berlin 1985, Chapt. 2.
[19] R. W. Munn, Low-Mobility Transport in Perfect Crystals, Ed. C. W. L. Goodman, Physics of Dielectric Solids, The Institute of Physics, Bristol 1980.
[20] I. G. Austin and N. F. Mott, Adv. Phys. **18,** 41 (1969).
[21] R. Blinc, G. Lahajnar, M. Pintar, and I. Zupancic, J. Chem. Phys. **44,** 1784 (1966).
[22] R. Blinc, S. Detoni, and M. Pintar. Phys. Rev. **124,** 1036 (1961).
[23] S. F. Hoffman and Szcepaniak, J. Mag. Rezonance **36,** 359 (1979).
[24] F. Y. Eithan, A. R. Bates, W. Gough, and D. J. Somerford, J. Phys. Condens. Matter **4,** L 249 (1992).
[25] S. Hoshino, Y. Okaya, and R. Pepinsky, Phys. Rev. **115,** 323 (1959).